Insect Biochemistry and Molecular Biology 130 (2021) 103519

Contents lists available at ScienceDirect

Insect Biochemistry and Molecular Biology

journal homepage: www.elsevier.com/locate/ibmb

Juvenile hormone induces methoprene-tolerant 1 phosphorylation to increase interaction with Taiman in *Helicoverpa armigera*

Yan-Xue Li, Di Wang, Wen-Li Zhao, Jun-Ying Zhang, Xin-Le Kang, Yan-Li Li, Xiao-Fan Zhao *

Shandong Provincial Key Laboratory of Animal Cells and Developmental Biology, School of Life Sciences, Shandong University, Qingdao, China

ARTICLE INFO

Keywords:
Basic-helix-loop-helix Per/Arnt/Sim protein
Methoprene-tolerant 1
Juvenile hormone
phosphorylation
Gene transcription

ABSTRACT

Methoprene-tolerant 1 (Met1) is a basic-helix-loop-helix Per/Arnt/Sim (bHLH-PAS) protein identified as the intracellular receptor of juvenile hormone (JH). JH induces phosphorylation of Met1; however, the phosphorylation site and outcomes of phosphorylation are not well characterized. In the present study, using the lepidopteran insect and serious agricultural pest *Helicoverpa armigera* (cotton bollworm) as a model, we showed that JH III induced threonine-phosphorylation of Met1 at threonine 393 (Thr393) in the Per-Arnt-Sim (PAS) B domain. Thr393-phosphorylation was necessary for Met1 binding to the JH response element (JHRE) to promote the transcription of *Kr-h1* (encoding transcription factor Krüppel homolog 1) because Thr393-phosphorylated Met1 increased its interaction with Taiman (Tai) and prevented the Met1-Met1 association. However, JH III could not prevent Met1-Met1 association after Met1-Thr393 was mutated, suggesting that Thr393-phosphorylation is an essential mechanism by which JH prevents Met1-Met1 association. The results showed that JH induces Met1 phosphorylation on Thr393, which prevents Met1-Met1 association, enhances Met1 interaction with Tai, and promotes the binding of Met1-Tai transcription complex to the E-box in the JHRE to regulate *Kr-h1* transcription.

1. Introduction

Juvenile hormone (JH) is a key hormone that maintains insect larval status (Riddiford, 2020). During insect development, JH prevents premature metamorphosis (Goodman and Cusson, 2012; Riddiford, 1994). The basic-helix-loop-helix Per/Arnt/Sim (bHLH-PAS) protein Methoprene-tolerant (Met) (Wilson and Fabian, 1986) functions as the JH intracellular receptor to maintain insect larval status (Charles et al., 2011; Miura et al., 2005). Met forms a JH-dependent heterodimeric transcription complex with SRC (p160/SRC, a steroid receptor coactivator also known as "FISC" or "Taiman/Tai") to initiate the transcription of *Kr-h1* (encoding transcription factor Krüppel homolog 1) by binding to its JH response element (JHRE) (Li et al., 2011; Zhu et al., 2003). Kr-h1 works downstream of Met and is induced rapidly by JH (Kayukawa et al., 2012; Minakuchi et al., 2009). Knockdown of *Met* caused precocious metamorphosis in *Tribolium castaneum* (Konopova and Jindra, 2007; Parthasarathy et al., 2008) and *Helicoverpa armigera* (Zhao et al., 2014). Met is an excellent target to develop insect growth regulators to control pest insects (Jindra and Bittova, 2019). Interestingly, Met forms a Met-Met complex in the coleopteran insect *T. castaneum* (Charles et al., 2011) and formed a heterodimer with another bHLH–PAS family member, Germ cells-expressed protein (Gce), when they were overexpressed in the S2 cells in the dipteran *Drosophila melanogaster* in the absence of the hormone (Godlewski et al., 2006). The Met-Met complex was dissociated by a conformational change in the presence of methoprene or JH III in *T. castaneum* and *D. melanogaster*, which promotes gene transcription (Jindra et al., 2015).

Phosphorylation of bHLH-PAS family members is widely observed, and is regulated by various kinase pathways (Kietzmann et al., 2016). Specific phosphorylation sites have been implicated in specific functional controls of these proteins (Gradin et al., 2002). In the mosquito, *Aedes aegypti*, Met was observed to be phosphorylated using two-dimensional electrophoresis (2-DE) of proteins after incubation with JH III via a phospholipase C (PLC) pathway (Liu et al., 2015), suggesting that JH III transmits a signal via a cell membrane signaling pathway to regulate Met for gene transcription. However, the

Abbreviations: JH, juvenile hormone; Met, Methoprene-tolerant; bHLH-PAS, basic-helix-loop-helix Per/Arnt/Sim; λPPase, lambda protein phosphatase; Kr-h1, Krüppel homolog 1; Tai, Taiman; JHRE, JH response element; E-box, motif in JHRE; Thr393, threonine residue at 393 in the protein; PLC, phospholipase C; PKC, protein kinase C; Phos-tag SDS-PAGE, phosphate-affinity sodium dodecyl sulfate–polyacrylamide gel electrophoresis; 2-DE, two-dimensional electrophoresis.

* Corresponding author.
E-mail address: xfzhao@sdu.edu.cn (X.-F. Zhao).

https://doi.org/10.1016/j.ibmb.2021.103519
Received 24 September 2020; Received in revised form 4 January 2021; Accepted 5 January 2021
Available online 13 January 2021

phosphorylation sites and outcomes have not been demonstrated.

In the present study, we identified the phosphorylation site of Met1 at Thr393 under JH III induction in *Helicoverpa armigera*. Thr393-phosphorylation could be detected using anti-phospho-threonine polyclonal antibodies, and its mobility variation was observed using Phos-tag SDS-PAGE followed by western blotting. Moreover, we revealed that Thr393-phosphorylation of Met1 promoted its interaction with Tai to form a transcription complex that promoted *Kr-h1* transcription. Thr393-phosphorylation of Met1 also prevented the Met1-Met1 association. These findings increase our understanding of the mechanism of bHLH-PAS protein interaction and function under hormonal regulation.

2. Results

2.1. JH III induced Met1 Thr-phosphorylation

To examine the extent and type of Met1 phosphorylation in *H. armigera*, we injected JH III into 6th instar 6 h larvae and examined the phosphorylation of Met1 using three kinds of antibodies, including anti-phospho-threonine polyclonal antibodies (Anti-pThr), anti-phospho-(Ser) PKC substrate polyclonal antibodies (Anti-pSer), and the anti-phosphotyrosine mouse monoclonal antibody 4G10 (Anti-pTyr). These antibodies recognize threonine-phosphorylation, PKC substrate serine-phosphorylation, and tyrosine-phosphorylation, respectively. Met1 was collected from the epidermis using polyclonal antibodies against *H. armigera* Met1. Only the Anti-pThr antibodies detected the target band, which was increased by JH III injection, compared with the basal levels in the dimethyl sulfoxide (DMSO) control, when the amount of Met1 was confirmed as equal. Lambda protein phosphatase (λPPase) treatment decreased the intensity of the Anti-pThr-detected band, suggesting that Met1 is a phosphorylated protein (Fig. 1A). The specificities of the antibodies were examined and confirmed (Fig. 1B).

To determine the profile of Thr-phosphorylation of Met1 during larval development, we examined Thr-phosphorylation of Met1 in the epidermis from fifth instar larvae to zero-day pupae by controlling Met1 loading after affinity purification. The levels of Thr-phosphorylated Met1 were higher at the sixth instar feeding stage (6th–24 h to 6th–48 h), then decreased during metamorphic molting (MM) (Fig. 1C), showing high levels of Thr-phosphorylated Met1 before metamorphosis.

The overexpression of Met1-RFP-His (a Met-red fluorescent protein (RFP)-His tag fusion protein) in an *H. armigera* epidermal cell line (HaEpi) produced similar results, and the RFP-His tag was not phosphorylated (Fig. 1D). These data suggested that Met1 is a threonine-phosphorylated protein *in vivo*, and JH III could increase the levels of Thr-phosphorylated Met1.

Phos-tag SDS-PAGE followed by western blotting was used to show the changes in protein mobility caused by Met1 phosphorylation. The anti-Met1 polyclonal antibodies detected three bands, comprising phospho-Met1, an unknown protein, and the non-phosphorylated Met1. The level of phospho-Met1 was low at the larval molting stage (5M), but high at the larval feeding stage (6th–24 h), and low at metamorphic stage (6th–96 h). The intensity of the phosphorylated protein band decreased after λPPase treatment, confirming it was a phospho-protein. Injection of JH III into 6th–6 h larvae increased the phospho-Met1 levels, compared with the Met1 in DMSO control, which was already phosphorylated *in vivo* (Fig. 1E), confirming that JH III increased Met1 phosphorylation. However, using Phos-tag SDS-PAGE, only a little phosphorylated-Met1 was detected, probably because of the limitation of the method; therefore, the levels of non-phosphorylated Met1 did not change correspondingly. Normal SDS-PAGE followed by western blotting, did not detect the mobility change of phosphor-Met1. These results confirmed the phosphorylation of Met1 under the JH III regulation *in vivo*.

2.2. JH III induced Met1 Thr393-phosphorylation in the PAC region

Various deletion mutants of Met1, M1 (▲HLH-Met1, 130–526 aa), M2 (▲C-Met1, 1–412 aa), M3 (▲PASB-C-Met1, 1–290 aa), M4 (▲HLH-PASA-Met1, 290–526 aa), M5 (PASB-Met1, 204–412 aa), and M6 (▲PAC-C-Met1, 1–359 aa) (Fig. 2A) were fused with RFP-His and overexpressed in HaEpi cells to determine the phosphorylated region of Met1. The anti-pThr antibodies detected Thr-phosphorylation of the wild-type Met1-RFP-His, M1, M2, M4, and M5. In contrast, phosphorylation of M3, M6, and RFP tags was not observed in the presence of JH III or DMSO treatment as a negative control (Fig. 2B). The data showed that JH III-induced Met1 Thr-phosphorylation occurs in the PAC region of Met1.

We further investigated the phosphorylation sites of Met1. The phosphorylation sites of Met1 were predicted using NetPhosK (http://www.cbs.dtu.dk/services/NetPhosK/) and NetPhos 3.1 Server (http://www.cbs.dtu.dk/services/NetPhos/), respectively, as references for site-directed mutation of Met1. The threonine at position 330 (score 0.81), serine at 367 (score 0.95), tyrosine at 369 (score 0.53), threonine at 393 (score 0.911), and serine at 404 (score 0.51) in the PASB domain were predicted as possible phosphorylation sites. Thr-phosphorylation of Met1 occurred in response to JH as defined above; therefore, the threonine residues at 330 and 393 are the most probable phosphorylation sites. The threonine residues at 330, 393, the serine residue at 367, and the tyrosine residue at 369 were replaced by alanine (T330A, T393A, S367A, and Y369A) to examine their contribution to Met1 Thr-phosphorylation under the control of JH III. The wild-type Met1-RFP-His displayed basal Thr-phosphorylation. The wild-type Met1-RFP-His, Met1-T330A-RFP-His, Met1-S367A-RFP-His, and Met1-Y369A-RFP-His showed an increase of Thr-phosphorylation levels under JH III induction. In contrast, the Thr-phosphorylation level of the Met1-T393A-RFP-His mutant was not increased significantly compared with that of the DMSO control (Fig. 2C), suggesting JH III increased Thr393-phosphorylation of Met1 over its basal threonine phosphorylation levels, and T393 is not the only phosphorylation site of Met1.

To confirm T393 phosphorylation by JH III regulation, we examined the mobility changes of the overexpressed-Met1-RFP-His and the mutant Met1-T393A-RFP-His using Phos-tag SDS-PAGE and western blotting. In the Phos-tag experiment, the anti-His monoclonal antibody detected the mobility shift from the phosphorylated-Met1 in wild-type Met1-RFP-His under JH III treatment, but not from the mutant Met1-T393A-RFP. In normal SDS-PAGE, the anti-His monoclonal antibody could not detect the mobility shift of phosphorylated-Met1 (Fig. 2D). These results confirmed that the phosphorylation of Met1 at T393 under JH III regulation.

2.3. Met1 phosphorylation at Thr393 determined its binding on JHRE for Kr-h1 transcription

To address the outcome of Met1 phosphorylation in the JH pathway, we examined the binding of Met1-RFP-His and Met1-T393A-RFP-His to JHRE (containing the E-box CACGTG) using a chromatin immunoprecipitation (ChIP) assay. This JHRE lies in the upstream region (−942 to −948) of *Kr-h1* in *H. armigera*. Using the primer for the JHRE of *Kr-h1* showed that Met1-RFP-His enriched more JHRE-containing fragments when exposed to JH III compared with that of DMSO control. Using primers for the CDS of *Kr-h1* that amplify the coding region of *Kr-h1* (*Kr-h1*-RTF and *Kr-h1*-RTR located in the cDNA) as a non-specific binding control, no JHRE-containing fragment was enriched under the same conditions (Fig. 3A), suggesting that Met1 phosphorylation is necessary for its binding to the JHRE. Meanwhile, *Kr-h1* transcripts were significantly increased under JH III regulation in Met1-RFP-His-overexpressing cells, but not in Met1-T393A-RFP-His-overexpressing cells (Fig. 3B), suggesting that Met1 phosphorylation is necessary for JH-induced *Kr-h1* transcription.

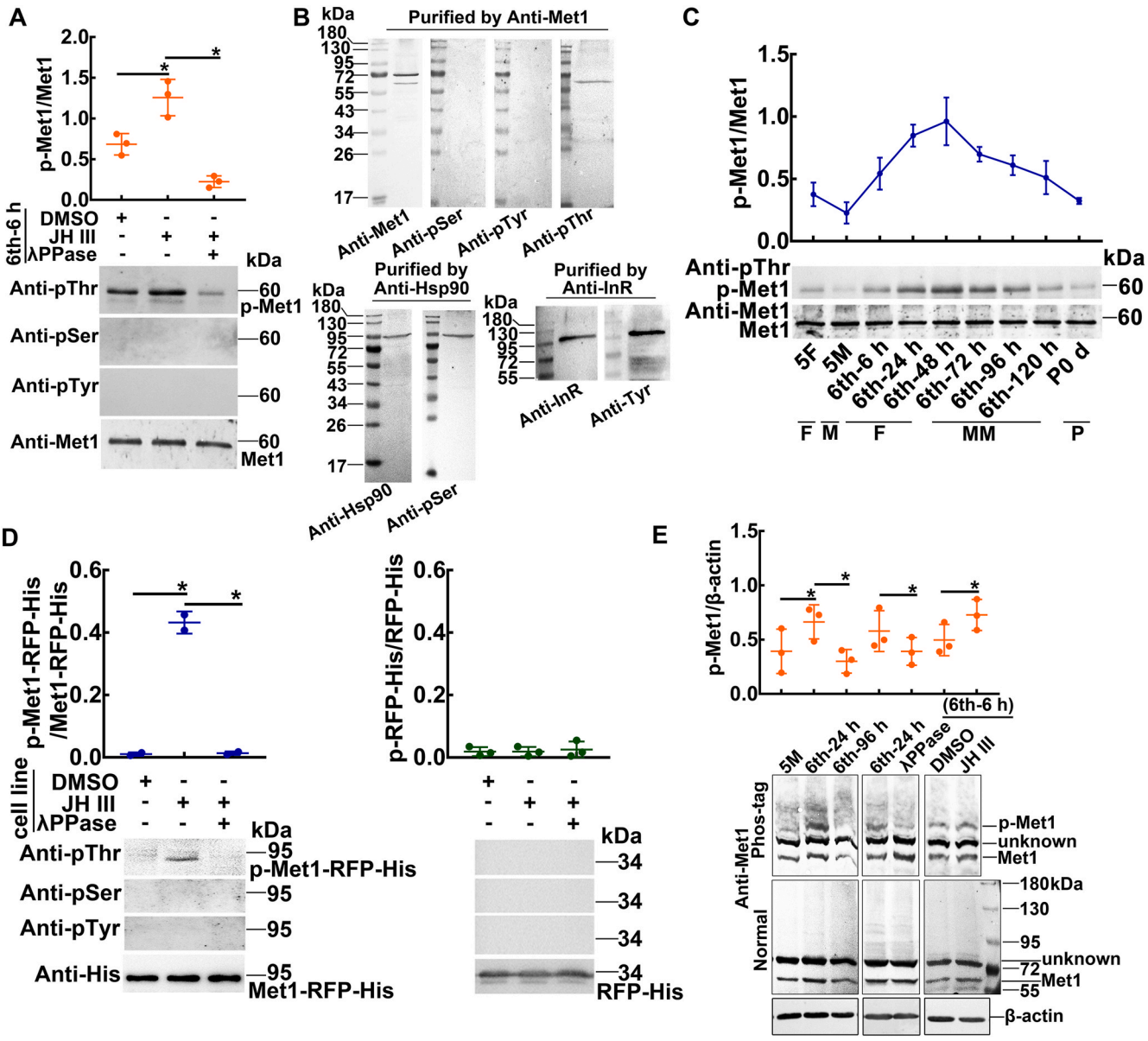

Fig. 1. Identification of Met1 phosphorylation. **A.** JH III triggers Thr-phosphorylation of Met1 in larvae. Met1 protein was enriched from the larval epidermis after JH III (500 ng/larva at 6th–6 h for 6 h) or DMSO treatment, using anti-Met1 antibodies-bound CNBr-activated Sepharose 4B. Met1 was detected using anti-Met1 rabbit polyclonal antibodies (prepared in our laboratory) as a loading control, and the phosphorylation of Met1 was detected using various antibodies such as anti-phospho-threonine polyclonal antibodies (Anti-pThr), anti-phospho-(Ser) PKC substrate polyclonal antibodies (Anti-pSer), and the anti-phosphotyrosine mouse monoclonal antibody 4G10 (Anti-pTyr). λPPase: samples treated with λ-phosphatase (0.5 μL λPPase in 50 μL buffer for 30 min at 30 °C). **B.** Examination of the specificity of the antibodies. Isolation of Met1 proteins using anti-Met1 polyclonal antibodies bound-CNBr-activated Sepharose 4B. The anti-pThr antibody recognized Met1. The anti-pSer antibody recognized Heat shock protein 90 (Hsp90) isolated by CNBr-activated Sepharose 4B with anti-Hsp90 polyclonal antibodies. The anti-pTyr antibody recognized insulin receptor (InR) isolated by protein A resin with anti-InR polyclonal antibodies. The proteins were extracted from 6 to 24 h larval epidermis. **C.** The Thr-phosphorylation level of Met1 in the epidermis during larval development. Met1 protein was isolated with the method detailed in (A), which normalized the Met1 protein levels. Met1 was detected using anti-Met1 antibodies as the loading control, and phosphorylation was detected using the anti-pThr antibodies. 5F: 5th -instar feeding larvae. 5M: 5th -instar molting larvae. 6th–24 h to 6th–120 h: 6th instar larvae at various stages. P0 d: new pupae. F: feeding. M: molting. MM: metamorphic molting. P: pupae. **D.** Overexpressed Met1 was threonine-phosphorylated under JH III induction in HaEpi cells. Overexpressed Met1-RFP-His or RFP-His in HaEpi cells for 48 h, followed by JH III (1 μM for 1 h) or DMSO treatment. Met1-RFP-His and RFP-His were isolated using His-binding-resin or anti-His antibody bound-CNBr-activated Sepharose 4B, and visualized using anti-His antibody as a loading control. The phosphorylation of Met1-RFP-His (94 kDa) was detected using anti-pThr antibodies, anti-pSer antibodies, and anti-pTyr antibodies. The secondary antibody was horseradish peroxidase-conjugated AffiniPure goat anti-rabbit or anti-mouse IgG. RFP-His was used as control. **E.** Detection of Met1 phosphorylation in the larval epidermis using anti-Met1 antibodies with Phos-tag SDS-PAGE and normal SDS-PAGE followed western blotting, respectively. 5M: fifth instar molting larvae; 6th–24 h: sixth instar 24 h larvae, 6th–96 h: sixth instar 96 h larvae. λPPase: 6th–24 h epidermis proteins were incubated with λPPase. The 6th instar 6 h larvae were injected with DMSO or JH III (500 ng/larva) for 6 h. β-actin was used as the loading control. The density of the immunoreactive protein bands on the Western blot was calculated using ImageJ software. Asterisks indicate significant differences between the groups ($^*p < 0.05$), as determined using the Student's *t*-test based on three independent experiments. Error bars indicate the standard deviation (SD) of three independent experiments.

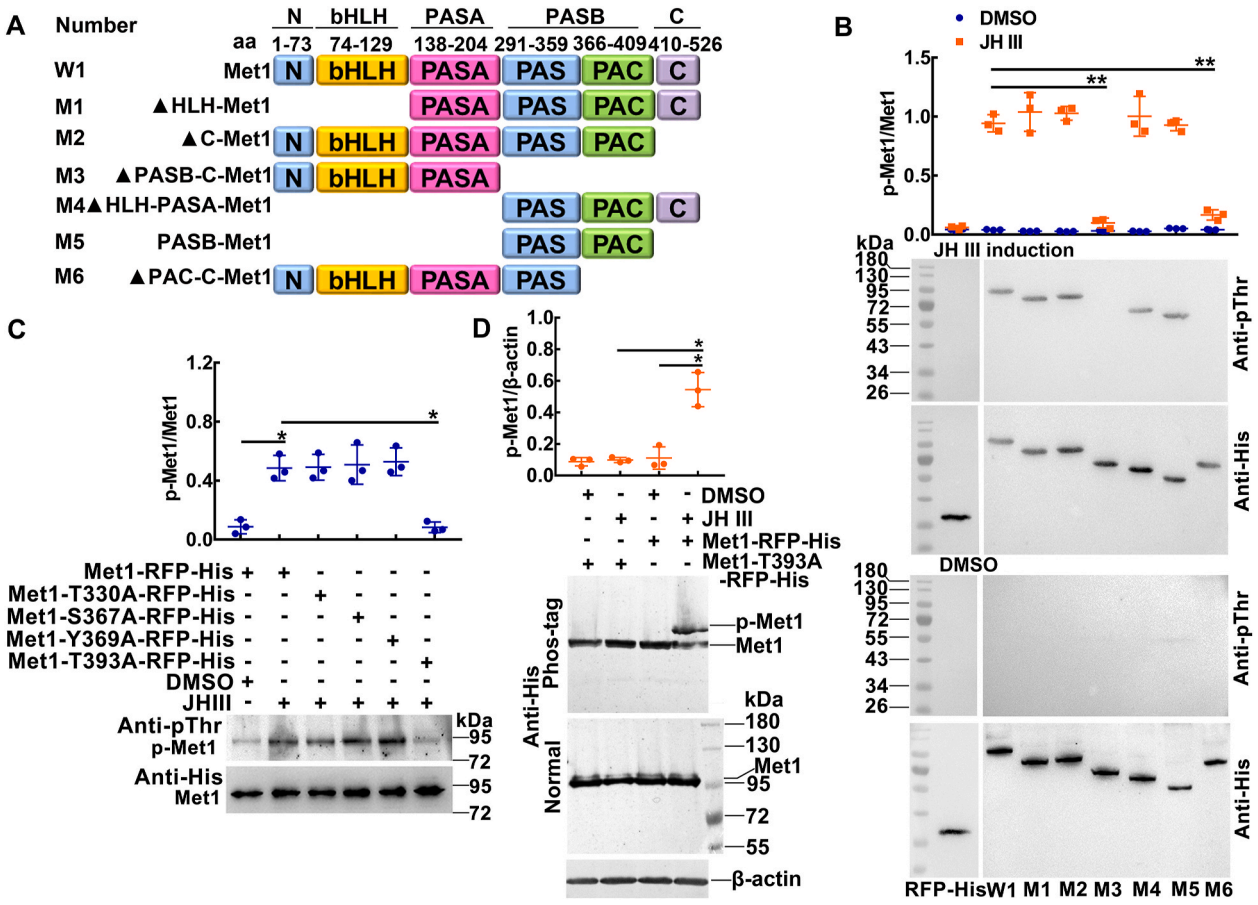

Fig. 2. Met1 was phosphorylated at T393 in the PAC region under JH III regulation. A. Chart was showing the truncated mutants of Met1. **B**. Detection of Thr-phosphorylation of Met1 and its mutants using western blotting with anti-pThr antibodies. Met1-RFP-His and the mutants were overexpressed in HaEpi cells for 48 h, then JH III (1 μM) or DMSO was administered for 1 h. The protein was isolated using anti-His antibody bound-CNBr-activated Sepharose 4B. An anti-His antibody detected Met1-RFP-His as a loading control. **C**. Site mutation to analyze Thr-phosphorylation residues of Met1. Met1-RFP-His and the site mutants were overexpressed, and the protein was isolated using anti-His antibody bound-CNBr-activated Sepharose 4B for detection. An anti-His antibody detected Met1-RFP-His as a loading control, and anti-pThr antibodies showed the phosphorylation level in wild-type Met1 and its mutants. **D**. Detection of phosphorylation of wild-type Met1 and the mutant T393 in HaEip cells using SDS-PAGE and Phos-tag SDS-PAGE, respectively. Phosphorylated and non-phosphorylated protein bands were displayed by the anti-His antibody. SDS-PAGE gel used for western blotting was a 7.5% gel. Quantification of the data by ImageJ; asterisks indicate significant differences between the groups ($*p < 0.05$), as determined by Student's *t*-test based on the SD of three independent experiments.

2.4. Met1 Thr393-phosphorylation increased the interaction with Tai and prevented Met1-Met1 association

To determine the mechanism by which Met1Thr393-phosphorylation promoted *Kr-h1* expression, we investigated the protein interactions. Tai-GFP-His and Met1-RFP-His, Tai-GFP-His and Met1-T393A-RFP-His, and GFP-His and RFP-His tags were paired and overexpressed in HaEpi cells, respectively, to explore the effect of Met1-Thr393 phosphorylation on its formation of transcription complexes. Input indicated the equal expression of the proteins. In Co-IP using the anti-GFP antibody, Met1-RFP-His not coprecipitated with Tai-GFP-His from the DMSO control; however, Met1-RFP-His was coprecipitated with Tai-GFP-His under JH III treatment, suggesting that Met1-RFP-His interacted with Tai-GFP-His. However, a low amount of Met1-T393A-RFP-His was coprecipitated with Tai-GFP-His under JH III treatment, suggesting the T393A mutation decreased the interaction with Tai-GFP-His (Fig. 4A). These results indicated that JH III-induced Met1-Thr393 phosphorylation promotes Met1 to recruit Tai to form a Met1-Tai transcription complex.

The Met1-RFP-His, Met1-GFP-His, Met1-T393A-RFP-His, and Met1-T393A-GFP-His constructs, were overexpressed in pairs in HaEpi cells, to further address the effect of Met1-Thr393 phosphorylation on Met1-Met1 interaction. In the DMSO control, Met1-GFP-His was coprecipitated with Met1-RFP-His using the antibody against RFP, and Met1-GFP-His was not coprecipitated with Met1-RFP-His in the presence of JH III, suggesting Met1 formed a Met1-Met1 complex that was dissociated by JH III treatment. However, JH III-induced dissociation of the Met1-Met1 complex was prevented when T393 was mutated (Fig. 4B). In the tag control, interaction of RFP-His and GFP-His was not detected either under DMSO or JH III treatment (Fig. 4C). These results suggested that JH III-induced Met1 phosphorylation at Thr393 prevents the association of the Met1-Met1 complex.

3. Discussion

bHLH-PAS proteins exert their transcriptional functions by forming homodimers or heterodimers; however, the regulatory mechanism is unclear. Using *H. armigera* as a model, we revealed that JH III induces Met1 Thr-phosphorylation at Thr393 in the PAC region of the PASB domain, which promoted Met1-Tai transcription complex formation and prevented Met1-Met1 association for *Kr-h1* transcription. Met1 Thr-phosphorylation occurred in growing larvae and decreased during metamorphosis.

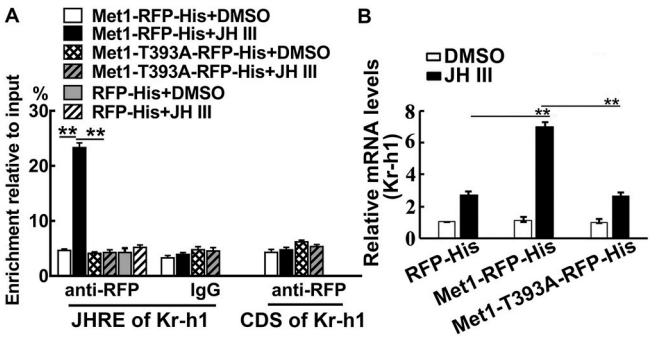

Fig. 3. Met1-T393 phosphorylation determines its transcription regulatory activity. **A**. qRT-PCR detected the JHRE fragment in the precipitate from chromatin immunoprecipitation (Ch-IP) produced using an anti-RFP antibody. Cells were transfected with the RFP-His (as a control), Met1-RFP-His, or Met1-T393A-RFP-His plasmids, and then incubated with JH III (1 μM, 3 h). IgG: Non-specific mouse IgG. anti-RFP: monoclonal antibody against RFP. Enrichment relative to input (%) (sample with IgG/input %) was calculated using a previously described formula (Sadasivam et al., 2012). Input: Samples before immunoprecipitation. CDS: coding sequence. **B**. qRT-PCR assay to detect *Kr-h1* transcripts. Cells were transfected with the RFP-His, Met1-RFP-His, or Met1-T393A-RFP-His plasmid, and then incubated with JH III (1 μM, 3 h); RFP-His was overexpressed as the tag control. *P*-value were obtained using Student's *t*-test based on three replicates (*$p < 0.05$; **$p < 0.01$).

3.1. JH III induces Met1 Thr393-phosphorylation in the PASB domain

Post-transcriptional modification of phosphorylation and dephosphorylation is a common mechanism that regulates many transcription factors. The specific site of phosphorylation is implicated in the specific functions of the protein (Gradin et al., 2002). For example, the phosphorylation of ecdysone receptor (EcR) at T468 by PKC delta under 20E regulation determines its transcriptional complex formation (Chen et al., 2017). Protein kinase D1 (PKD1)-mediated phosphorylation at Thr324 in the PASB domain of hypoxia-inducible factor-2α (HIF-2α) promotes genomic instability (To et al., 2006). The pinpoint phosphorylation of T393 after HaMet1 was treated with JH was not clear; however, the specific recognition of the amino acid motif around the site of the substrate by a protein kinase is one of the mechanisms of protein pinpoint phosphorylation (van de Kooij et al., 2019).

Multiple phosphorylated forms of *A. aegypti* Met were induced by JH III, as observed using 2-dimensional electrophoresis of proteins (Liu et al., 2015); however, to identify the phosphorylation site was a challenge, because the NetPhosK or NetPhos 3.1 software predicted many phosphorylation sites in the Met1 protein. The phospho-(Ser) PKC substrate antibody did not detect AaMET phosphorylation after JH application in *A. aegypti* (Ojani et al., 2016). We also did not detect phosphorylation of Met1 using phospho-(Ser) PKC substrate antibodies. However, we detected Thr-phosphorylation of Met1 and identified the site at Thr393 in the PAC region of the PASB domain under JH III regulation. Some basal levels of Met1 Thr-phosphorylation were detected in DMSO-treated wild-type Met1-RFP-His and JH III-treated Met1--T393A-RFP-His mutant expressing cells, suggesting that Met1 has constitutive threonine phosphorylation on other sites, which should be determined in a future study. Thr393 is conserved in the Met proteins of most lepidopteran insects and *Drosophila* GCE, but not in Met of *Drosophila*, *Tribolium* and *A. aegypti*, as determined by aligning the Met proteins of *Helicoverpa armigera* Met1: AHX26585.1, *Manduca sexta* Met: XP_030020305.1 *Danaus plexippus* Met1: OWR52183, *Bombyx mori* Met1: BAJ05085.1, *Plutella xylostella* Met1: XP_011557479, *Drosophila melanogaster* Gce: NP_001188593.1, *Drosophila melanogaster* Met1: AHN59602.1, *Aedes aegypti* Met: AAX55681.1, and *T. castaneum* Met: NP_001092812.1 (Fig. S1). There is a possibility that JH induces Met1 phosphorylation on other residues in different insects, which needs to be addressed in future work using other antibodies or methods.

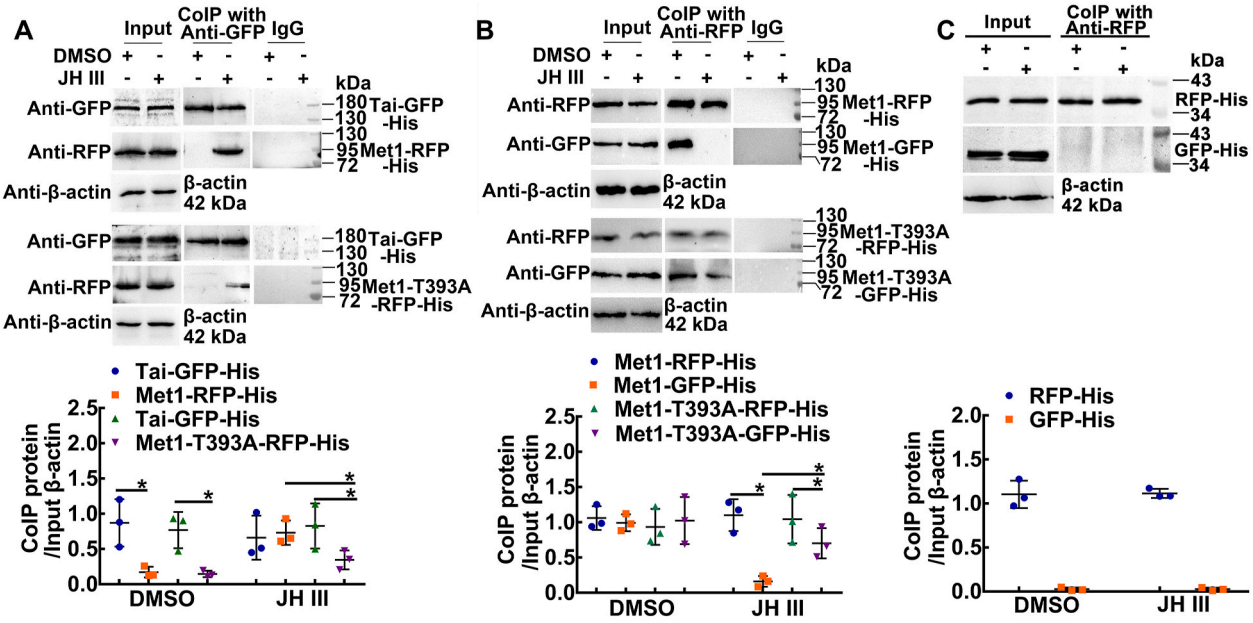

Fig. 4. Met1-T393 phosphorylation dependent protein–protein interactions. A. Phosphorylation of Met1-T393 promoted the interaction of Met1 with Tai under JH III regulation. Transfected cells were treated with 1 μM JH III or DMSO for 3 h, and then proteins were extracted. Input: Protein levels of Tai-GFP-His, Met1-RFP-His, and Met1-T393A-RFP-His in cells before co-immunoprecipitation (Co-IP), detected using an antibody against GFP or RFP. Co-IP: anti-GFP antibody-immunoprecipitated Tai-GFP-His, co-immunoprecipitated Met1-RFP-His, or Met1-T393A-RFP-His, detected using an anti-GFP or anti-RFP monoclonal antibody. Nonspecific IgG was used as a negative control. **B**. Dissociation of the wild-type Met1-GFP-His and Met1-RFP-His complex under JH III regulation. Met-T393A-GFP-His and T393A-RFP-His mutants did not dissociate under JH III regulation. Input: Samples before co-immunoprecipitation (Co-IP). CoIP: Met1-RFP-His and Met1-T393A-RFP-His were immunoprecipitated using an anti-RFP **monoclonal** antibody. Met1-GFP-His and Met1-T393A-GFP-His were detected using an anti-GFP **monoclonal** antibody. Transfected cells were treated with JH III (1 μM for 3 h) or DMSO. **C.** RFP-His and GFP-His as negative tag controls for A and B. The significance of the difference between the two groups are shown by the *P*-value, based on Student's *t*-test of three independent experiments (*$p < 0.05$; **$p < 0.01$).

3.2. Met1 Thr393-phosphorylation increases Met1-Tai interaction and is necessary for its transcriptional function

JH, via its intracellular receptor Met, regulates various biological processes at different stages of the insect life cycle, including growth in *D. melanogaster* larvae (Mirth et al., 2014), reproductive maturation in *T. castaneum* (Parthasarathy et al., 2010), and preventing pupation or adult emergence in *B. mori* (Guo et al., 2012). Met1 forms a transcriptionally active complex with another bHLH-PAS protein termed Tai or Src in *T. castaneum* (Zhang et al., 2011) and FISC in mosquitoes (Li et al., 2011). Met-Tai complexes bind E-boxes (CACGTG) in the upstream region of *Kr-h1* genes in *Tribolium*, *Drosophila*, *Apis* (Kayukawa et al., 2012), and *H. armigera* (Zhao et al., 2014) to promote their transcription. Kr-h1 mediates the anti-metamorphic effect of JH across distant insect orders (Minakuchi et al., 2008).

In *A. aegypti*, the phosphorylation of MET and/or TAI is essential for the binding of its complex to the JHRE (Liu et al., 2015). Ojani et al. found that the binding of JH-induced AaMET-AaTAI to the JHRE of AaET was dramatically repressed when inhibited a specific PKC inhibitor. Our results further revealed that JH III-induced Met1 Thr393-phosphorylation is critical for Met1's interaction with Tai for *Kr-h1* transcription. These studies suggested that the intrinsic signaling pathway in insect cells is vital for Met1 phosphorylation and function in a JH-dependent manner. A previous study showed that BmMet1/BmSRC and TcMet/TcSRC increased the activity of a kJHRE reporter but elicited only a weak JH response in HEK293 cells (Kayukawa et al, 2012, 2013; Kayukawa and Shinoda, 2015), indicating some differences between insect cells and mammal cells. However, in mammalian HEK293 cells, Met1 is capable of forming a functional JH receptor complex with SRC in the presence of JH and thus activates kJHRE, suggesting that JH might activate certain components, such as certain kinases, which are evolutionarily conserved components in insects, followed by the regulation of the phosphorylation of Met/Tai, thereby triggering weak JHRE reporting activity.

3.3. Met1 Thr393-phosphorylation prevents Met1-Met1 association

The "Met-Met homodimer" and "Met-Gce heterodimer" were identified after overexpressing the proteins in the S2 cells of *Drosophila* (Godlewski et al., 2006). A Met-Met dimer was also reported in the absence of JH in yeast and insect L57 cells (Bitra and Palli, 2009). The stoichiometry of the Met-Met dimer has not been determined; therefore, the term "Met-Met complex" was used by later authors (Charles et al., 2011). In *T. castaneum*, JH III caused Met-Met dissociation via a conformational change of Met after binding JH (Charles et al., 2011). We also observed that JH III induced Met-Met complex dissociation; however, the mechanism appears to act via Thr393-phosphorylation of Met1. Mutation of Thr393 abrogated JH III-induced Met-Met complex dissociation, which presents a new JH-induced Met dissociation mechanism.

3.4. The profile of Thr-phosphorylation of Met1

The levels of Thr-phosphorylated Met1 were higher at the sixth instar feeding stage, then decreased during metamorphic molting, suggesting JH promotes Thr-phosphorylation of Met1, and 20E represses Thr-phosphorylation of Met1. The titer of JH I in the hemolymph of *Bombyx* showed peaks at the 3rd and 4th instar larvae, and rapidly decreased to the low level before ecdysis. A repeat of the increase in JH titer occurred at the time of the final stage of the fifth larvae (Furuta et al., 2013; Niimi and Sakurai, 1997). The 20E titer increases during metamorphosis in the whole body (Kang et al., 2019) and the hemolymph (Di et al., 2020) in *H. armigera*. 20E counteracts JH function in regulating protein phosphorylation in *H. armigera* (Pan et al., 2018). Thus, the crosstalk between JH and 20E determines the levels of Met1 phosphorylation.

Although JH I and JH II are natural hormones for lepidopteran larvae (Furuta et al., 2013; Schooley et al., 1984), *H. armigera* and *B. mori* (Deng et al., 2011; Kayukawa et al., 2012) respond to JH III (the commercially available form of JH) as well. In *B. mori* Bm-aff3 cells, the effective concentration of JHs to induce *Kr-h1* transcription, JH I, JH II, JH III, JHA, or methyl farnesoate were 1.6×10^{-10}, 1.2×10^{-10}, 2.6×10^{-10}, 6.0×10^{-8}, and 1.1×10^{-7} M, respectively (Kayukawa et al., 2012). In cultures of wing imaginal discs of *B. mori*, 1–2 μM JH III promoted cuticle protein 4 gene expression (Deng et al., 2011). The effective concentration of JH III to induce rapid calcium increase in *H. armigera* HaEpi cells is $\geq$ 1 μM (Wang et al., 2016).

4. Conclusion

JH III regulates Met1 phosphorylation at Thr393 in the PAC region of the PASB domain. Thr393-phosphorylation of Met1 prevents the Met1-Met1 association and enhances the Met1-Tai interaction to form a transcription complex. The Met1-Tai complex binds to the JHRE to induce *Kr-h1* transcription to maintain the larval status (Fig. 5).

5. Materials and methods

5.1. Insects

The cotton bollworms, *Helicoverpa armigera*, obtained from the Henan Agricultural University in China, were fed an artificial diet comprising soybean powder, wheat germ with various vitamins, and mineral salt. The insects were maintained in an insectarium under the cycle of 14 h light: 10 h dark at 26 ± 1 °C with 60%–70% humidity.

5.2. Cell culture

Our laboratory established an *H. armigera* epidermal cell line (HaEpi), which was obtained from the *H. armigera* epidermis (Shao et al., 2008). The cells were cultured at 27 °C with a loosely attached monolayer in tissue culture flasks. The tissue culture flasks had an area of 25 cm^2 and contained 5 mL of antibiotic-free Grace's medium supplemented with 10% certified fetal bovine serum (Biological Industries, Cromwell, CT, USA). When the cells developed into a near confluent monolayer they were sub-cultured.

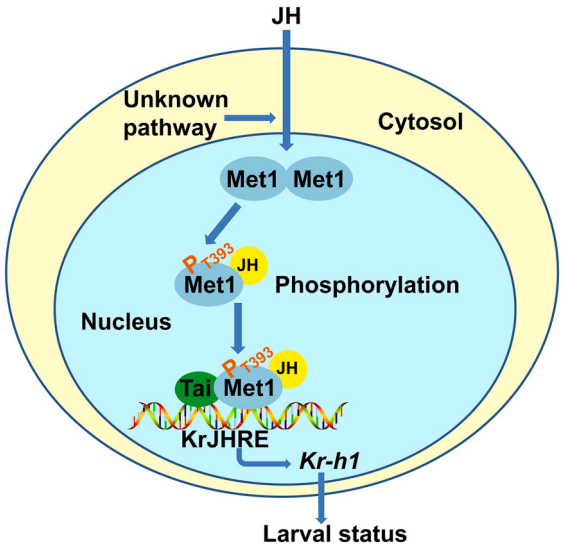

Fig. 5. A schematic diagram showing the role of Met1 Thr393-phosphorylation in the JH pathway. JH III induces phosphorylation of Met1 at Thr393, which promotes the separation of the Met1-Met1 complex, thus enhancing Met1's interaction with Tai to form a transcription complex, which binds to a JHRE to activate *Kr-h1* transcription.

5.3. Overexpression of proteins in HaEpi cells

The nucleotide sequence of the *Met1* or *Tai* was cloned into the pIEx-4-His plasmid (Novagen, Pretoria, South Africa) and fused with the green fluorescent protein (GFP) or red fluorescent protein (RFP) using specific primers. HaEpi cells were cultured to 80% density at 27 °C in Grace's medium supplemented with 10% FBS. Next, recombinant plasmid (5 μg) and sterilized saline solution (200 μL) medium containing transfection reagent (8–16 μL) were mixed with Grace's medium (2 mL) according to the supplier's instructions (Biodragon, Beijing, China) and incubated with cells for 48 h.

5.4. Western blotting

Total proteins were extracted from tissues using Tris-HCl buffer (40 mM Tris-buffered saline, pH 7.5), or from cells using RIPA lysis buffer (Radioimmunoprecipitation assay lysis buffer) with a Protease Cocktail and Phosphatase Inhibitor (EDTA-free) (Yi Sheng Biological Technology Co., Ltd., Shanghai, China). The supernatant was collected and the protein concentration was determined using a BCA Protein Assay Kit (Beyotime Biotechnology, Shanghai, China). The proteins were mixed with sodium dodecylsulfate polyacrylamide gel electrophoresis (SDS-PAGE) loading buffer, and boiled for 10 min. Next, the protein sample was subjected to 7.5–12.5% SDS-PAGE and then electrophoretically transferred onto nitrocellulose membranes. The membranes were incubated in blocking buffer (3–5% fat-free powdered milk in TBS (10 mM Tris-HCl, 150 mM NaCl, pH 7.5)) at room temperature for 1 h. The primary antibodies used for these assays were diluted in blocking buffer, followed by incubation at 37 °C for 4 h or overnight at 4 °C. The membrane was subsequently washed three times with TBST (0.02% Tween in TBS) for 10 min each time, followed by the addition of alkaline phosphatase-conjugated or horseradish peroxidase-conjugated AffiniPure horse anti-rabbit or anti-mouse IgG secondary antibody (ZSGB-BIO, Beijing, China), diluted 1:5,000 with the same blocking buffer. The immunoreactive proteins were visualized using NBT (p-nitro-blue tetrazolium chloride, 100 mg/mL in 70% dimethylformamide) and BCIP (5-bromo-4-chloro-3-indolyl phosphate, 50 mg/mL in 100% dimethylformamide) diluted in TBS (1:200) in the dark for 10 min, or Peroxide buffer and Luminol/Enhancer Solution were mixed at a 1:1 ratio, added to the blot, and incubated for 1 min. The blot was exposed to the Chemiluminescence imaging system (Tanon, Shanghai, China) after the excess reagent was drained off and covered with a clear plastic sheet. The molecular masses of the immunoreactive proteins were estimated using their theoretically calculated sizes (https://web.expasy.org/compute_pi/) and their gel mobility in comparison to the standard proteins.

5.5. Identification of phosphorylation of Met1

The endogenous Met1 protein was isolated from the larval tissue homogenates using RIPA buffer (50 mM Tris-HCl, 150 mM NaCl, 1% TritonX-100, 0.1% SDS, Beyotime Biotechnology), and the protein was purified using anti-Met1 rabbit polyclonal antibodies (prepared in our laboratory) that were bound to CNBr-activated Sepharose 4B. The recombinant plasmid containing wild-type Met1 and those with the mutant fused with pIEx-4-RFP-His were overexpressed in HaEpi cells for 48 h, followed by treatment with JH III (1 μM) for 1 h or an equivalent amount of diluted DMSO as a control. Proteins were extracted from the cells using 500 μL of RIPA Lysis Buffer, and isolated using anti-His mouse monoclonal antibody His bound-CNBr-activated Sepharose 4B or His-binding-resin. The proteins were subjected to 7.5–12.5% SDS-PAGE, and then electrophoretically transferred onto nitrocellulose membranes. The membranes were incubated in blocking buffer (5% bovine serum albumin in TBS) for 1 h at room temperature. Then, the membranes were incubated with the primary antibodies: anti-phospho-Threonine polyclonal antibodies (ImmuneChem Pharmaceuticals, Burnaby, British Columbia, Canada), anti-phospho-(Ser) PKC substrate polyclonal antibodies (Cell Signaling Technology, Danvers, MA, USA), and an anti-phospho-(Tyr) mouse monoclonal antibody 4G10 (Biodragon, Beijing, China) diluted in blocking buffer (1:2000) at 4 °C overnight, respectively. The membranes were washed three times with TBST for 10 min each time, followed by the addition of the horseradish peroxidase conjugated AffiniPure goat anti-rabbit or anti-mouse IgG secondary antibody, diluted 1:5000 with the same blocking buffer. The protein bands were visualized using High-Sig ECL Western Blotting Substrate and observed using a Chemiluminescence imaging system (Tanon, Shanghai, China), according to the manufacturer's instruction manual.

5.6. Isolation of proteins using antibody bound-CNBr-activated Sepharose 4B

The antibodies (50 μL anti-Met1 polyclonal antibodies or 10 μL anti-His monoclonal antibody) were dialyzed in coupling buffer (0.1 M $NaHCO_3$, 0.5 M NaCl, pH 8.3) overnight at 4 °C. CNBr-activated Sepharose 4B (60 mg) was dissolved in 500 μL of 1 mM HCl. After washing with 1 mM HCl three times, the dialyzed antibody was added to CNBr-activated Sepharose 4B and incubated for 2 h with gentle shaking at room temperature. After washing five times with the coupling buffer, the column was incubated with Tris-HCl (0.1 M, pH 8.0) for 1 h at room temperature. The column contents were washed four times with acetic acid buffer (0.1 M sodium acetate, 0.5 M NaCl, pH 4.0) and TBS buffer (0.1 M Tris-HCl, 0.5 M NaCl, pH 8.0), and then the column was washed with TBS buffer (0.1 M Tris-HCl, 0.1 M NaCl, pH 8.0) before use. Proteins were extracted using RIPA lysis buffer and harvested via centrifugation at 12,000×*g* for 20 min at 4 °C. Approximately 30–40 μL of supernatant was used as the protein input. The remaining supernatant was added to the treated column and incubated with gentle shaking at 4 °C overnight. Next, the column was washed with TBS buffer, followed by protein elution using 200 μL of 0.1 M glycine (pH 2.5) and 10 μL Tris-HCl (1 M, pH 8.0). The eluted proteins were treated with SDS-PAGE loading buffer and boiled for 10 min for western blotting analysis.

5.7. Lambda phosphatase (λPPase) treatment

The protein was extracted from the larvae and cells using RIPA lysis buffer with EDTA-free. A 40-μL sample of the protein (0.1 mg/mL) was subsequently incubated with 0.5 μL of λPPase, 5 μL of buffer, and 5 μL of $MnCl_2$ at 30 °C for 30 min, according to the manufacturer's specifications (New England Biolabs Beijing LTD, Beijing, China). The proteins were then subjected to SDS-PAGE, followed by western blotting analysis. Using antibodies recognizing phosphorylated and non-phosphorylated proteins.

5.8. Mutation of Met1

Deletion-mutants of Met1, M1 (▲HLH-Met1, 130–526 aa), M2 (▲C-Met1, 1–412 aa), M3 (▲PASB-C-Met1, 1–290 aa), M4 (▲HLH-PASA-Met1, 290–526 aa), M5 (PASB-Met1, 204–412 aa) and M6 (▲PAC-C-Met1, 1–359 aa) were produced by reverse transcription PCR (RT-PCR). The cDNA fragments were fused with RFP-His and overexpressed in HaEpi cells from plasmid pIEx-4-His plasmid (Novagen). The cDNA sequence of the site mutations was produced by bridged-RT-PCR. Then, the cDNA fragment was inserted into pIEx-4-His plasmid where they were fused with the RFP tag.

5.9. Chromatin immunoprecipitation assay (Ch-IP)

Met1-RFP-His and Met1-T393A-RFP-His were overexpressed in HaEpi cells. After 48 h of culture, the cells incubated with 1 μM JH III for 3 h. The cells were then cross-linked using 1% formaldehyde and harvested in 300 μL of lysis buffer (50 mM HEPES, pH 7.5, 140 mM NaCl,

1% Triton X-100, protease, and phosphatase inhibitors). DNA in the solution was broken into fragments via sonication, and three replicate samples were prepared by diluting 100 μL of DNA supernatant in 900 μL of dilution buffer (16.7 mM Tris-HCl, pH 8.1, 167 mM NaCl, 0.01% SDS, and 1.1% Triton X-100). Protein A agarose beads (10 μL) were added to the DNA supernatant for pre-treatment nonspecific binding. After centrifugation, one supernatant sample was used as a negative control input for quantitative real-time PCR (qRT-PCR). Other supernatants were incubated with anti-RFP antibody or IgG at 4 °C overnight. Protein A agarose beads pretreated with dilution buffer were mixed with the negative control sample or the antibody-antigen-chromatin mixture. After the beads were washed, eluted (elution buffer: 1% SDS, 0.1 M $NaHCO_3$), and reverse cross-linked (65 °C overnight), RNase and Protease K were added to clear RNA and proteins, respectively. The DNA was isolated via phenol/chloroform extraction and used as the template for qRT-PCR to detect the JHRE fragment in the *Kr-h1* promoter region using the JHREF1 and JHRER1 primers (HKr-h1-F and HKr-h1-R). RFP-His was overexpressed simultaneously in HaEpi cells as tagged negative controls for the fusion proteins. Enrichment of the input (%) = (sample precipitated by the antibody-sample with IgG)/input % was calculated using a previously described method (Sadasivam et al., 2012).

5.10. Co-immunoprecipitation (Co-IP)

The recombinant plasmids Met1-RFP-His and Tai-GFP-His, Met1-GFP-His and Met1-RFP-His, Met1-T393A-RFP-His and Met1-T393A-GFP-His were co-transfected into HaEpi cells when they reached a density of 80%. After 48 h, the cells were incubated with JH III (1 μM) or DMSO. Proteins were extracted from the cells using 500 μL of RIPA Lysis Buffer with 5 μL Protease Cocktail and Phosphatase Inhibitor (EDTA-free) and harvested via centrifugation at 12,000×*g* for 15 min at 4 °C. Forty microliters of supernatant were used as the protein input. The remaining supernatant was added to a monoclonal antibody targeting GFP, RFP, or IgG and incubated overnight with gentle shaking at 4 °C. Protein A resin was added to the supernatant to eliminate non-specific binding, followed by immediate centrifugation. The supernatant was incubated with Protein A resin for a further 3 h with gentle shaking at 4 °C. After centrifugation at 3,000×*g* for 5 min at 4 °C, the supernatant was discarded. After washing with 500 μL of RIPA lysis buffer three times, the resin was treated with SDS-PAGE loading buffer and boiled for 10 min for western blotting analysis. The primary antibodies used for Co-IP were mouse monoclonal antibody against GFP and RFP (ABclonal, Wuhan, China). GFP-His and RFP-His were overexpressed in the HaEpi cells as tag controls.

5.11. Phos-tag SDS-PAGE

Phos-tag SDS-PAGE was performed by mixing Phos-tag Acrylamide (20 μM; Fujifilm Wako Pure Chemical Corporation, Osaka, Japan) and $MnCl_2$ (80 μM) into a normal SDS-PAGE gel. The phosphates of the phospho-proteins can bind Mn^{2+} to decrease their mobility in the gel. Protein samples were precipitated using 20% trichloroacetic acid (TCA) to remove the chelating agent from the sample. The proteins were transferred from Phos-tag SDS-PAGE gel to nitrocellulose membranes for western blotting after removing Mn^{2+} by incubating the gel in transfer buffer with 10 mmol/L EDTA for 10 min for three times with shaking.

5.12. Statistical analysis

The densities of the protein bands on the western blots were quantified using ImageJ software (NIH, Bethesda, MA, USA). GraphPad Prism 7 was used for data analysis (GraphPad Software Inc., La Jolla, CA, USA). All data were from at least three biologically independent experiments. Two-group datasets were analyzed using Student's *t*-test. In the figures, asterisks indicate significant differences between the groups ($^*p < 0.05$, $^{**}p < 0.01$). The details are provided in the related figure legends. Error bars indicate the standard deviation (SD) of three independent experiments.

5.13. Antibodies

The present study used anti-phospho-Threonine polyclonal antibodies (ImmuneChem Pharmaceuticals, Burnaby, British Columbia, Canada), anti-phospho-(Ser) PKC substrate polyclonal antibodies (Cell Signaling Technology, Danvers, MA, USA), anti-phospho-(Tyr) mouse monoclonal antibody 4G10 (Beijing Biodragon Immunotechnologies Co., Ltd, Beijing, China), anti-Met1 polyclonal antibodies (Prepared in our laboratory), anti-GFP monoclonal antibody, anti-RFP monoclonal antibody, anti-His monoclonal antibody, anti-β-actin polyclonal antibodies (ABclonal, Wuhan, China).

Author contributions

Y.-X. L. did most of the experiments. D. W. and W.-L. Z. did some experiments in Fig. 2. J.-Y. Z. performed the qRT-PCR. X.-L. K. analyzed Met1 structure. Y.-L. L. provided data in Fig. 1B. X.-F. Z. designed the study and wrote the final version of the manuscript.

Declaration of competing interest

The authors declare that they have no conflicts of interest with the contents of this article.

Acknowledgments

We thank Professor Lynn M. Riddiford, member of the National Academy of Sciences, for her advice in the study and revision of the manuscript. This study was supported by the National Natural Science Foundation of China (grant no. 31730083).

Appendix A. Supplementary data

Supplementary data to this article can be found online at https://doi.org/10.1016/j.ibmb.2021.103519.

References

Bitra, K., Palli, S.R., 2009. Interaction of proteins involved in ecdysone and juvenile hormone signal transduction. Arch. Insect Biochem. Physiol. 70, 90–105. https://doi.org/10.1002/arch.20281.

Charles, J.P., Iwema, T., Epa, V.C., Takaki, K., Rynes, J., Jindra, M., 2011. Ligand-binding properties of a juvenile hormone receptor, Methoprene-tolerant. Proc. Natl. Acad. Sci. U. S. A 108, 21128–21133. https://doi.org/10.1073/pnas.1116123109.

Chen, C.H., Pan, J., Di, Y.Q., Liu, W., Hou, L., Wang, J.X., Zhao, X.F., 2017. Protein kinase C delta phosphorylates ecdysone receptor B1 to promote gene expression and apoptosis under 20-hydroxyecdysone regulation. Proc. Natl. Acad. Sci. U. S. A 114, E7121–E7130. https://doi.org/10.1073/pnas.1704999114.

Deng, H., Zheng, S., Yang, X., Liu, L., Feng, Q., 2011. Transcription factors BmPOUM2 and BmβFTZ-F1 are involved in regulation of the expression of the wing cuticle protein gene BmWCP4 in the silkworm, Bombyx mori. Insect Mol. Biol. 20, 45–60. https://doi.org/10.1111/j.1365-2583.2010.01041.x.

Di, Y.Q., Han, X.L., Kang, X. Le, Wang, D., Chen, C.H., Wang, J.X., Zhao, X.F., 2020. Autophagy triggers CTSD (cathepsin D) maturation and localization inside cells to promote apoptosis. Autophagy 1–23. https://doi.org/10.1080/15548627.2020.1752497, 00.

Furuta, K., Ichikawa, A., Murata, M., Kuwano, E., Shinoda, T., Shiotsuki, T., 2013. Determination by LC-MS of juvenile hormone titers in hemolymph of the silkworm, bombyx mori. Biosci. Biotechnol. Biochem. 77, 988–991. https://doi.org/10.1271/bbb.120883.

Godlewski, J., Wang, S., Wilson, T.G., 2006. Interaction of bHLH-PAS proteins involved in juvenile hormone reception in Drosophila. Biochem. Biophys. Res. Commun. 342, 1305–1311. https://doi.org/10.1016/j.bbrc.2006.02.097.

Goodman, W.G., Cusson, M., 2012. The Juvenile Hormones. In: Gilbert, L.I.B.T.-I.E. (Ed.), Insect Endocrinology. Academic Press, San Diego, pp. 310–365. doi:10.1016/B978-0-12-384749-2.10008-1.

Gradin, K., Takasaki, C., Fujii-Kuriyama, Y., Sogawa, K., 2002. The transcriptional activation function of the HIF-like factor requires phosphorylation at a conserved threonine. J. Biol. Chem. 277, 23508–23514. https://doi.org/10.1074/jbc.M201307200.

Guo, E., He, Q., Liu, S., Tian, L., Sheng, Z., Peng, Q., Guan, J., Shi, M., Li, K., Gilbert, L.I., Wang, J., Cao, Y., Li, S., 2012. MET is required for the maximal action of 20-hydroxyecdysone during Bombyx metamorphosis. PloS One 7. https://doi.org/10.1371/journal.pone.0053256.

Jindra, M., Bellés, X., Shinoda, T., 2015. Molecular basis of juvenile hormone signaling. Curr. Opin. Insect Sci. 11, 39–46. https://doi.org/10.1016/j.cois.2015.08.004.

Jindra, M., Bittova, L., 2019. The juvenile hormone receptor as a target of juvenoid "insect growth regulators. Arch. Insect Biochem. Physiol. 103, 1–7. https://doi.org/10.1002/arch.21615.

Kang, X. Le, Zhang, J.Y., Wang, D., Zhao, Y.M., Han, X.L., Wang, J.X., Zhao, X.F., 2019. The steroid hormone 20-hydroxyecdysone binds to dopamine receptor to repress lepidopteran insect feeding and promote pupation. PLoS Genet. https://doi.org/10.1371/journal.pgen.1008331.

Kayukawa, T., Minakuchi, C., Namiki, T., Togawa, T., Yoshiyama, M., Kamimura, M., Mita, K., Imanishi, S., Kiuchi, M., Ishikawa, Y., Shinoda, T., 2012. Transcriptional regulation of juvenile hormone-mediated induction of Krüppel homolog 1, a repressor of insect metamorphosis. Proc. Natl. Acad. Sci. U. S. A 109, 11729–11734. https://doi.org/10.1073/pnas.1204951109.

Kayukawa, T., Shinoda, T., 2015. Functional characterization of two paralogous JH receptors, methoprene-tolerant 1 and 2, in the silkworm, Bombyx mori (Lepidoptera: bombycidae). Appl. Entomol. Zool. 50, 383–391. https://doi.org/10.1007/s13355-015-0345-8.

Kayukawa, T., Tateishi, K., Shinoda, T., 2013. Establishment of a versatile cell line for juvenile hormone signaling analysis in Tribolium castaneum. Sci. Rep. 3, 1–9. https://doi.org/10.1038/srep01570.

Kietzmann, T., Mennerich, D., Dimova, E.Y., 2016. Hypoxia-Inducible Factors (HIFs) and phosphorylation: impact on stability, localization, and transactivity. Front. Cell Dev. Biol. 4, 1–14. https://doi.org/10.3389/fcell.2016.00011.

Konopova, B., Jindra, M., 2007. Juvenile hormone resistance gene Methoprene-tolerant controls entry into metamorphosis in the beetle Tribolium castaneum. Proc. Natl. Acad. Sci. U. S. A 104, 10488–10493. https://doi.org/10.1073/pnas.0703719104.

Li, M., Mead, E.A., Zhu, J., 2011. Heterodimer of two bHLH-PAS proteins mediates juvenile hormone-induced gene expression. Proc. Natl. Acad. Sci. U. S. A 108, 638–643. https://doi.org/10.1073/pnas.1013914108.

Liu, P., Peng, H.J., Zhu, J., 2015. Juvenile hormone-activated phospholipase C pathway enhances transcriptional activation by the methoprene-tolerant protein. Proc. Natl. Acad. Sci. U. S. A 112, E1871–E1879. https://doi.org/10.1073/pnas.1423204112.

Minakuchi, C., Namiki, T., Shinoda, T., 2009. Krüppel homolog 1, an early juvenile hormone-response gene downstream of Methoprene-tolerant, mediates its anti-metamorphic action in the red flour beetle Tribolium castaneum. Dev. Biol. 325, 341–350. https://doi.org/10.1016/j.ydbio.2008.10.016.

Minakuchi, C., Zhou, X., Riddiford, L.M., 2008. Krüppel homolog 1 (Kr-h1) mediates juvenile hormone action during metamorphosis of Drosophila melanogaster. Mech. Dev. 125, 91–105. https://doi.org/10.1016/j.mod.2007.10.002.

Mirth, C.K., Tang, H.Y., Makohon-Moore, S.C., Salhadar, S., Gokhale, R.H., Warner, R.D., Koyam, T., Riddiford, L.M., Shingleton, A.W., 2014. Juvenile hormone regulates body size and perturbs insulin signaling in Drosophila. Proc. Natl. Acad. Sci. U. S. A 111, 7018–7023. https://doi.org/10.1073/pnas.1313058111.

Miura, K., Oda, M., Makita, S., Chinzei, Y., 2005. Characterization of the Drosophila Methoprene-tolerant gene product: juvenile hormone binding and ligand-dependent gene regulation. FEBS J. 272, 1169–1178. https://doi.org/10.1111/j.1742-4658.2005.04552.x.

Niimi, S., Sakurai, S., 1997. Development changes in juvenile hormone and juvenile hormone acid titers in the hemolymph and in vitro juvenile hormone synthesis by corpora allata of the silkworm, Bombyx mori. J. Insect Physiol. 43, 875–884. https://doi.org/10.1016/S0022-1910(97)00021-8.

Ojani, R., Liu, P., Fu, X., Zhu, J., 2016. Protein kinase C modulates transcriptional activation by the juvenile hormone receptor methoprene-tolerant. Insect Biochem. Mol. Biol. 70, 44–52. https://doi.org/10.1016/j.ibmb.2015.12.001.

Pan, J., Di, Y.Q., Li, Y.B., Chen, C.H., Wang, J.X., Zhao, X.F., 2018. Insulin and 20-hydroxyecdysone oppose each other in the regulation of phosphoinositide-dependent kinase-1 expression during insect pupation. J. Biol. Chem. 293, 18613–18623. https://doi.org/10.1074/jbc.RA118.004891.

Parthasarathy, R., Sun, Z., Bai, H., Palli, S.R., 2010. Juvenile hormone regulation of vitellogenin synthesis in the red flour beetle, Tribolium castaneum. Insect Biochem. Mol. Biol. 40, 405–414. https://doi.org/10.1016/j.ibmb.2010.03.006.

Parthasarathy, R., Tan, A., Palli, S.R., 2008. bHLH-PAS family transcription factor methoprene-tolerant plays a key role in JH action in preventing the premature development of adult structures during larval-pupal metamorphosis. Mech. Dev. 125, 601–616. https://doi.org/10.1016/j.mod.2008.03.004.

Riddiford, L.M., 2020. Rhodnius, golden oil, and Met: a history of juvenile hormone research. Front. Cell Dev. Biol. 8, 1–18. https://doi.org/10.3389/fcell.2020.00679.

Riddiford, L.M., 1994. Cellular and molecular actions of juvenile hormone I. General considerations and premetamorphic actions. Adv. Insect Physiol 24, 213–274. https://doi.org/10.1016/S0065-2806(08)60084-3.

Sadasivam, S., Duan, S., DeCaprio, J.A., 2012. The MuvB complex sequentially recruits B-Myb and FoxM1 to promote mitotic gene expression. Genes Dev. 26, 474–489. https://doi.org/10.1101/gad.181933.111.

Schooley, D.A., Baker, F.C., Tsai, L.W., Miller, C.A., Jamieson, G.C., 1984. Juvenile hormones O, I, and II exist. In: Hoffmann, J., Porchet, M. (Eds.), Only in Lepidoptera BT - Biosynthesis, Metabolism and Mode of Action of Invertebrate Hormones. Springer Berlin Heidelberg, Berlin, Heidelberg, pp. 373–383.

Shao, H.L., Zheng, W.W., Liu, P.C., Wang, Q., Wang, J.X., Zhao, X.F., 2008. Establishment of a new cell line from lepidopteran epidermis and hormonal regulation on the genes. PloS One 3. https://doi.org/10.1371/journal.pone.0003127.

To, K.K.W., Sedelnikova, O.A., Samons, M., Bonner, W.M., Huang, L.E., 2006. The phosphorylation status of PAS-B distinguishes HIF-1α from HIF-2α in NBS1 repression. EMBO J. 25, 4784–4794. https://doi.org/10.1038/sj.emboj.7601369.

van de Kooij, B., Creixell, P., van Vlimmeren, A., Joughin, B.A., Miller, C.J., Haider, N., Linding, R., Stambolic, V., Turk, B.E., Yaffe, M.B., 2019. Comprehensive Substrate Specificity Profiling of the Human Nek Kinome Reveals Unexpected Signaling Outputs. Elife. https://doi.org/10.1101/515221.

Wang, D., Pei, X.Y., Zhao, W.L., Zhao, X.F., 2016. Steroid hormone 20-hydroxyecdysone promotes higher calcium mobilization to induce apoptosis. Cell Calcium 60, 1–12. https://doi.org/10.1016/j.ceca.2016.05.003.

Wilson, T.G., Fabian, J., 1986. A Drosophila melanogaster mutant resistant to a chemical analog of juvenile hormone. Dev. Biol. 118, 190–201. https://doi.org/10.1016/0012-1606(86)90087-4.

Zhang, Z., Xu, J., Sheng, Z., Sui, Y., Palli, S.R., 2011. Steroid receptor co-activator is required for juvenile hormone signal transduction through a bHLH-PAS transcription factor, methoprene tolerant. J. Biol. Chem. 286, 8437–8447. https://doi.org/10.1074/jbc.M110.191684.

Zhao, W.L., Liu, C.Y., Liu, W., Wang, D., Wang, J.X., Zhao, X.F., 2014. Methoprene-tolerant 1 regulates gene transcription to maintain insect larval status. J. Mol. Endocrinol. 53, 93–104. https://doi.org/10.1530/JME-14-0019.

Zhu, J., Chen, L., Raikhel, A.S., 2003. Posttranscriptional control of the competence factor βFTZ-F1 by juvenile hormone in the mosquito Aedes aegypti. Proc. Natl. Acad. Sci. U. S. A 100, 13338–13343. https://doi.org/10.1073/pnas.2234416100.